Chemical Process Design Vol.3 No.1 (2024) 1-15

University of Sistan and Baluchestan

Chemical Process Design

Available online at http://cpd.usb.ac.ir/

The Modified Picard Iteration Method for Solving the Moving Boundary Problems with a Dissolution Term Encountered in the Drug Release Systems

Mahmoodreza Rahimi*, Ruhollah Fazli-Abukheyli

Department of Chemical Engineering, Yasouj University, Yasouj 75918-74831, Iran

ARTICLE INFO

Article history:
Received: 2023-11-21
Received in revised form: 2024-01-03
Accepted: 2024-02-13
Published online: 2024-02-15

Keywords:
Modified Picard iteration method; Moving boundary problem; Dirichlet boundary conditions; Approximate solution; Drug release

DOI: *10.22111/cpd.2024.47529.1031*

ABSTRACT

The primary goal of this work is to develop an accurate analytical solution for the moving boundary problems with a dissolution term encountered in drug release from nanoporous structures. To achieve this, we propose applying the modified Picard iteration method for the first time. Using this approach, the moving boundary problem with Dirichlet boundary conditions is transformed into a single integral and then solved iteratively by selecting a suitable starting function. To validate the proposed method, we first analyze the behavior of the equations in specific cases. For these examples, the modified Picard iteration method provides more accurate results than the Picard iteration method, the variational iteration method, and the Adomian decomposition method. Furthermore, the solutions obtained from the proposed method satisfy both boundary conditions, whereas other iterative approaches do not fulfill one of the boundary conditions. The proposed method is also verified by comparing its results with experimental data on drug release from halloysite tubules reported in the literature. The findings indicate that simultaneous dissolution from the moving interface and the perimeter of the pores may be a possible mechanism for drug release from the halloysite tubules.

1. Introduction

The Stefan problems, or moving boundary problems, occur in many natural and industrial phenomena. Since prior information about the position of the moving interface is not known and it must be determined as part of the solution, such problems are inherently nonlinear [1–3]. Mathematically, solving moving boundary problems is significantly complicated, and exact analytical solutions are restricted to a limited number of specific cases [4]. Therefore, extensive research has been conducted on developing approximate numerical and analytical methods to solve these problems.

Corresponding author. Tel.: +98 9177168295
E-mail address: mrrahimi@yu.ac.ir (M. Rahimi).

In the literature, various numerical methods have been successfully applied to solve moving boundary problems [5–10]. Despite the prevalence of numerical approaches, facilitated by the availability of high-speed computers, approximate analytical solutions remain valuable. The advantage of approximate analytical methods over numerical ones is that they are generally much easier to use and explicitly show the dependency relationships between variables [11]. Some approximate analytical methods reported in the literature for solving moving boundary problems include the pseudo-steady state method [4,12], perturbation method [13,14], integral balance method [15–17], refined integral balance method [18,19], coupled integral equations approach [20], integral iterative formulation [21,22], homotopy perturbation method [23–25], Adomian decomposition method [26,27], and variational iteration method [26,28]. Recently, Witula et al. [29, 30] have applied Picard's iterative method to solve one-phase and two-phase Stefan problems. In this method, an iterative relation is formulated to find the temperature distribution in the given domain. The position of the moving interface is also approximated as a linear combination of some base functions, with the coefficients of this combination calculated by minimizing a properly constructed function.

Over the past decades, the mathematical analysis of moving boundary problems encountered in controlled release systems has garnered considerable attention. Higuchi [31] was the pioneer in analyzing this problem for drug release from matrix systems under sink conditions. Subsequently, Paul and McSpandden [32] derived an expression for drug release under sink conditions by adopting the exact solution of the classical Stefan problem. Lee [33] presented approximate analytical solutions for drug release from polymeric matrices with perfect sink and constant, finite external volume conditions. Abdekhodaie and Cheng [34] obtained an exact solution for drug release from planar and spherical systems into a finite external volume. Cohen and Erneux [35] solved Higushi's model for cases where the drug solubility in the matrix is a prescribed function of time. Jain et al. [36] present an analytical solution for drug release from a bioerodible spherical capsule through a transformation that converts the moving boundary problem into a fixed boundary problem. Garshasbi et al. [37] studied the nonlinear moving boundary problem in drug release from a swellable polymeric spherical platform. They used an iterative procedure based on the backward finite difference method to solve the problem numerically.

Recently, the authors proposed a mechanism to describe drug release from nanoporous structures and modeled it mathematically as a moving boundary problem with a dissolution term [12]. They solved this problem using the pseudo-steady state method (PSSA), under the assumption of low drug solubility. While the PSSA can simplify calculations, it may not yield applicable results, where steady-state assumptions do not hold, particularly when the initial drug loading is below its solubility. Therefore, the primary objective of this study is to extend the previous work of the authors [12] by developing a more accurate analytical solution. To achieve this, we propose to apply the modified Picard iteration method [38] to solve moving boundary problems with Dirichlet boundary conditions. To the best of our knowledge, the modified Picard iteration method has not been used for solving moving boundary problems. To assess the validity of the modified Picard iteration method, we compare the results obtained for some specific cases with those from the exact solution, the Picard iteration method, the variational iteration method, and the Adomian decomposition method. We also discuss the applicability of our proposed method by comparing it with experimental data on drug release from nanoporous structures reported in the literature.

2. Method

2.1. Mathematical formulation of the problem

When the drug is loaded above its solubility into porous structures, a molecular coating (strongly bound) forms on the internal surface of the pores, while crystals of the drug (weakly bound) accumulate on top of the strongly bound molecular layer and inside the pores [39,40]. When soaked in the release medium, the weakly bound crystals dissolve quickly, creating a moving interface, while the strongly bound molecules remain on the surface of the pore and dissolve at a slower rate (Fig. 1). If the pore diameter is large, the amount of drug released from the surface of the pores is negligible compared to the amount released from the moving interface. However, when the pore diameter is small, the amount of drug released from the surface of the pores increases due to the enhancement of the specific surface area. In this situation, the dissolution of the drug from the surface of the pores may affect the release rate and, therefore, must be considered in the mathematical modeling of the release process.

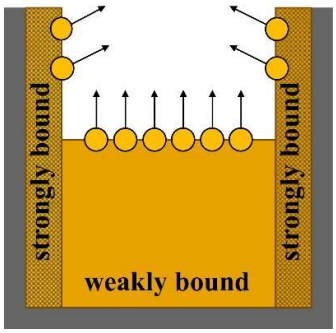

Fig. 1. Schematic representation of moving boundary problem with a dissolution term

Consider a non-erodible porous system containing a drug that its molecular size is small compared to the pore size. Assuming that (i) the diffusion of the drug through the pores is one-dimensional, and (ii) the dissolution rate from the perimeter of the pores follows a Noyes-Whitney type equation, the moving boundary problem with a dissolution term for describing the drug release from liquid-filled pores is given by the following equation [12]:

$$\frac{\partial c'(x',t')}{\partial t'} = D\frac{\partial^2 c'(x',t')}{\partial x'^2} - k'\left(c'(x',t') - c_s\right), 0 < x' < s'(t) \tag{1}$$

The conditions at the fixed and moving interfaces, respectively, are as follows:

$$c'(0,t') = f'(t) \tag{2}$$

$$c'(s',t') = c_s \tag{3}$$

The position of the moving interface is determined by:

$$\frac{ds'(t')}{dt'} = \frac{D}{\rho}\frac{\partial c'(x',t')}{\partial x'}\bigg|_{x'=s'(t')} \tag{4}$$

with the initial condition:

$$s'(0) = 0 \tag{5}$$

In the above equations, *t'* represents time, *c'* is the drug concentration, c_s is the drug solubility in the release medium, *x'* is the spatial coordinate, *s'*(*t*) is the moving interface position, ρ is the solid drug density, *D* is the diffusion coefficient and *k'* is the interfacial dissolution rate constant. Both *D* and *k'* are assumed to have constant values. Choosing *L* as a reference length and setting:

$$t=\frac{Dt'}{L^2},x=\frac{x'}{L},s=\frac{s'}{L},c=\frac{c'-c_s}{c_s},k=\frac{L^2k'}{D},f\left(t\right)=\frac{f'\left(t\right)-c_s}{c_s} \tag{6}$$

the problem is rescaled into the following form:

$$\frac{\partial c\left(x,t\right)}{\partial t}=\frac{\partial^2 c\left(x,t\right)}{\partial x^2}-kc\left(x,t\right),0<x<s\left(t\right) \tag{7}$$

$$c\left(0,t\right)=f\left(t\right) \tag{8}$$

$$c\left(s,t\right)=0 \tag{9}$$

$$\frac{ds\left(t\right)}{dt}=Ste\left.\frac{\partial c\left(x,t\right)}{\partial x}\right|_{x=s(t)} \tag{10}$$

$$s\left(0\right)=0 \tag{11}$$

where Ste=cs/ρ is the Stefan number.

After solving the problem, the amount of drug released per unit interface area is determined by solving the following equation:

$$\frac{dM\left(t\right)}{dt}=\left.\frac{\partial c}{\partial x}\right|_{x=0} \tag{12}$$

2.2. Modified Picard iteration method

Consider the following one-phase, one-dimensional moving boundary problem with a zero initial condition and a time-dependent Dirichlet boundary condition:

$$\frac{\partial u\left(x,t\right)}{\partial t}=\frac{\partial^2 u\left(x,t\right)}{\partial u^2}-ku\left(x,t\right),0<x<s\left(t\right) \tag{13}$$

$$u\left(0,t\right)=f\left(t\right) \tag{14}$$

$$u\left(s,t\right)=0 \tag{15}$$

$$\frac{ds\left(t\right)}{dt}=-\alpha\left.\frac{\partial u\left(x,t\right)}{\partial x}\right|_{x=s(t)} \tag{16}$$

$$s\left(0\right)=0 \tag{17}$$

where α is a constant corresponding to the Stefan number.

Rearranging Eq. (13), we get:

$$\frac{\partial^2 u\left(x,t\right)}{\partial x^2}=\frac{\partial u\left(x,t\right)}{\partial t}+ku\left(x,t\right) \tag{18}$$

As claimed in [38], Eq. (18) is integrated twice partially with respect to x, and then, the double integral is transformed into the following single integral:

$$u(x,t)=\int_0^x (x-z)\left(\frac{\partial u(z,t)}{\partial t}+ku(z,t)\right)dz+ax+b \tag{19}$$

Eq. (19) is solved now iteratively by choosing

$$u_0(x,t)=f(t)\left(1-\frac{x}{s(t)}\right) \tag{20}$$

as a starting function that satisfies both boundary conditions in Eqs. (14) and (15). This function is then substituted into the right-hand side of Eq. (19). After integration and applying the boundary conditions, we obtain $u_1(x,t)$. By repeating the iterative process, we achieve the following recurrence formula to obtain $u_{m+1}(x,t)$ from $u_m(x,t)$:

$$u_{m+1}(x,t)=\int_0^x (x-z)\left(\frac{\partial u_m(z,t)}{\partial t}+ku_m(z,t)\right)dz+ax+b, m=0,1,2,3,... \tag{21}$$

According to the modified Picard iteration method [38], the arbitrary constants, a and b, in Eq. (21) are re-evaluated at the end of each iteration by applying the boundary conditions given in Eqs. (14) and (15). The iteration process is repeated until the required degree of accuracy is attained.

To find the moving interface position, the obtained result for $u(x,t)$ is differentiated with respect to x at $x=s$, then substituted into Eq. (16). The solution of the governed ordinary differential equation in the first iteration leads to the following general formula for the position of the moving interface:

$$s_1(t)=\sqrt{\frac{6\alpha\int_0^t \frac{f(\tau)g(\tau)}{\alpha f(\tau)+3}d\tau}{g(t)}} \tag{22}$$

where

$$g(t)=exp\left(\alpha\int_0^t \frac{\left(kf(\tau)+\frac{df(\tau)}{d\tau}\right)}{\alpha f(\tau)+3}d\tau\right) \tag{23}$$

In the second iteration and beyond, except for a few specific cases, the governed ODE has no exact analytical solution. In this situation, the position of the moving interface can be determined using appropriate methods available in the literature [26,29,30].

3. Results and discussion

To validate the modified Picard iterative method (MPIM), we first analyze the behavior of the equations in specific cases. Then, the usefulness of this method is ascertained by comparing its results with experimental drug release profiles reported in the literature. All computations are performed using GNU Octave software, version 8.3.0.

3.1. Comparisons of specific cases

In this subsection, the obtained results for three specific cases are compared to those obtained using the exact solution, the Picard iteration method (PIM), the variational iteration method (VIM), and the Adomian decomposition method (ADM). The recurrence formula of VIM, PIM, and ADM, along with their solutions for $u(x,t)$ and $s(t)$ after one iteration, are presented in the Appendix. It should be noted that both VIM and PIM yield the same result for $u(x,t)$, and all VIM, PIM, and ADM provide the same result for $s(t)$.

3.1.1. Case 1

In the case that k=0, $f(t)$=1 and α=*Ste*, the problem defined by Eqs. (13)-(17) admits the exact solution of the classical Stefan problem:

$$u(x,t) = 1 - \frac{erf\left(\eta \frac{x}{s}\right)}{erf(\eta)} \tag{24}$$

$$s(t) = 2\eta\sqrt{t} \tag{25}$$

where the value of η is determined by solving the following equation:

$$\sqrt{\pi}\eta exp\left(\eta^2\right) erf(\eta) = Ste \tag{26}$$

The solution of the classical Stefan problem using MPIM is obtained as follows:

after one iteration:

$$u_1(x,t) = 1 - \left(\frac{\eta_1^2}{12} + 1\right)\left(\frac{x}{s}\right) + \left(\frac{\eta_1^2}{12}\right)\left(\frac{x}{s}\right)^3 \tag{27}$$

$$s_1(t) = 2\eta_1\sqrt{t} \tag{28}$$

$$\eta_1 = \sqrt{\frac{6Ste}{Ste+3}} \tag{29}$$

after two iterations:

$$u_2(x,t) = 1 - \left(\frac{\eta_2^4}{1440} + \frac{\eta_2^2}{12} + 1\right)\left(\frac{x}{s}\right) + \left(\frac{\eta_2^4}{144} + \frac{\eta_2^2}{12}\right)\left(\frac{x}{s}\right)^3 - \frac{\eta_2^4}{160}\left(\frac{x}{s}\right)^5 \tag{30}$$

$$s_2(t) = 2\eta_2\sqrt{t} \tag{31}$$

$$\eta_2 = \frac{\sqrt{6Ste\left(5Ste + 15 - \sqrt{225 + 150Ste - 15Ste^2}\right)}}{2Ste} \tag{32}$$

As can be seen, the results of MPIM for $u(x,t)$ are polynomials of the odd power of x, similar to the expansion of the “erf” function. Fig. 2 shows $u(x,t)$ obtained from the iterative approaches (one iteration only) with the exact solution at two different times for Ste=0.1 and 1.0. It is observed that the results of the present method are indistinguishable from the exact results for these values of Stefan number. However, other techniques (PIM, VIM, ADM) agree with the exact solution only for *Ste*=0.1 and exhibit deviations from the exact formula for *Ste*=1.0. It is seen from Fig. 2b that these deviations increase with time. Additionally, Fig. 2 shows that the results of MPIM satisfy both boundary conditions, while, for *Ste*=1.0, PIM and VIM overestimate at $x=s$ and ADM underestimates at

x=0. The difference between the results of MPIM and other methods can be attributed to the fact that in PIM, VIM, and ADM, the boundary conditions are applied only once in the starting function, whereas in MPIM, there are two arbitrary constants that are reassessed at the end of each iteration through the application of the boundary conditions.

Eqs. (28) and (31) demonstrate that the obtained solution for the moving interface position varies as the square root of time, similar to the exact solution (Eq. (25)); however, its dependency on the Stefan number (*Ste*) is not the same as for the exact one. This is shown in more detail in Table 1. In this table, the moving interface position obtained by one and two iterations of MPIM is compared with those obtained by the exact solution and other iterative methods. Again, an excellent agreement between the results of MPIM and the exact solution is observed. It is evident that for large Stefan numbers, the results of the MPIM are significantly improved by increasing the iteration number. Table 1 shows that PIM, VIM, and ADM provide accurate results only for relatively small Stefan numbers and deviate from the exact solution when this parameter increases.

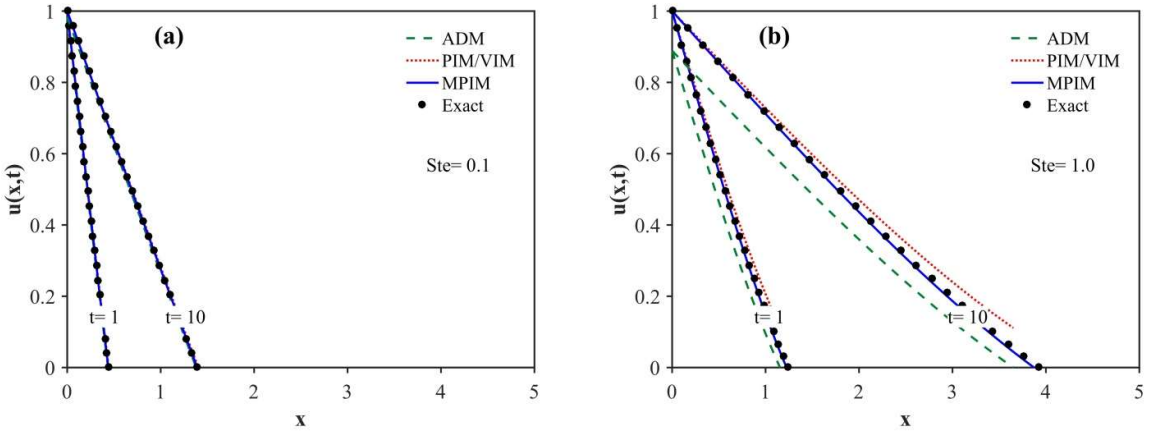

Fig. 2. Results of $u(x,t)$ versus x at different times for the case in which k=0, $f(t)$=1 and α=*Ste*. (a) *Ste*=0.1, (b) *Ste*=1.0

Table 1. Comparison of $s(t)/\sqrt{t}$ determined from different approaches for various Stefan numbers for the case in which k=0, $f(t)$=1 and, α=*Ste*

Ste	**Exact**	**MPIM**				**PIM/VIM/ADM**			
		m=1	Error (%)	m=2	Error (%)	m=1	Error (%)	m=2	Error (%)
0.05	0.3136	0.3136	0.01	0.3136	0.01	0.3124	-0.40	0.3124	-0.39
0.10	0.4400	0.4399	-0.01	0.4400	0.01	0.4364	-0.81	0.4367	-0.75
0.50	0.9296	0.9258	-0.41	0.9297	0.01	0.8944	-3.78	0.9037	-2.79
1.00	1.2401	1.2247	-1.24	1.2408	0.06	1.1547	-6.89	1.1904	-4.01

3.1.2. Case 2

For the problem in which k=0, $f(t)$=exp(t)-1 and α=1, the exact solutions are given by the following equations [6]:

$$u(x,t) = exp(t-x) - 1 \tag{33}$$

$$s(t) = t \tag{34}$$

For such a problem, MPIM provides the following results after one iteration:

$$u_1(x,t)=exp(t)-1+\left(\frac{\left(6+s^2\right)exp(2t)+3s^2exp(t)-6}{4\left(2+exp(t)\right)s}\right)x+\frac{exp(t)}{2}x^2 + \left(\frac{\left(2-s^2\right)exp(2t)-\left(4+s^2\right)exp(t)+2}{4\left(2+exp(t)\right)s^3}\right)x^3 \quad (35)$$

$$s_1(t)=\sqrt{\frac{6\left(exp(t)-t-1\right)}{exp(t)+2}} \quad (36)$$

The results for $u(x,t)$ obtained from the approximate methods and the exact solution are plotted in Fig. 3. Observe that, whereas MPIM is in good agreement with the exact solution at t=0.1 and 0.5, other methods fit the exact formula relatively well only at t=0.1 and show significant deviations at t=0.5. It can also be seen that the results of MPIM satisfy both boundary conditions at x=0 and x=s, whereas other iterative methods do not fulfill one of the boundary conditions.

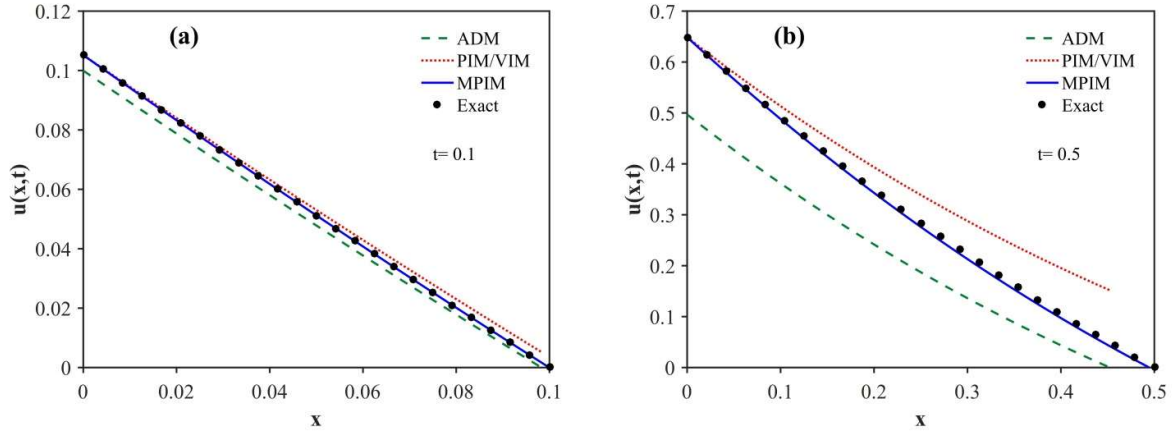

Fig. 3. Results of $u(x,t)$ versus x for the case in which k=0, $f(t)$=$exp(t)$-1 and α=1. (a) t=0.1, (b) t=0.5

For the moving interface position, a comparison of the exact value with the approximate ones obtained by MPIM and other iterative approaches is shown in Fig. 4. As observed, PIM, VIM, and ADM agree well with the exact result only at t<0.3, while there is good agreement between our proposed method and the exact solution at t<0.8. Expanding the right-hand side of Eq. (36) gives:

$$s_1(t)=t-\frac{1}{24}t^3-\frac{1}{180}t^4+\ldots \quad (37)$$

which indicates that we should take the exact solution in initial times.

3.1.3. Case 3

For the case of k=1, $f(t)$=-1, α=-Ste and $Ste\rightarrow 0$ (small Stefan number), the problem is solved analytically using the pseudo-steady state assumption (PSSA) as follows [12]:

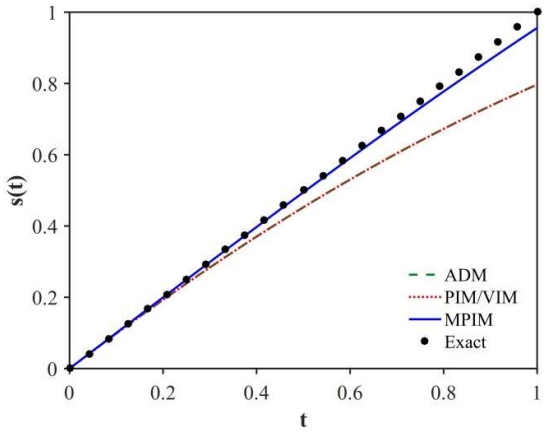

Fig. 4. Results of $s(t)$ versus t for the case in which k=0, $f(t)$=$exp(t)$-1 and α=1

$$u(x,t)=\frac{sinh(x-s)}{sinh(s)} \tag{38}$$

$$s(t)=cosh^{-1}(1+Ste.t) \tag{39}$$

Using MPIM (one iteration) for solving this problem, we obtain the following results:

$$u_1(x,t)=-1+\left(\frac{s}{3}+\frac{1}{s}\right)x-\left(\frac{1}{2}\right)x^2+\left(\frac{1}{6s}\right)x^3 \tag{40}$$

$$s_1(t)=\sqrt{6\left(1-exp\left(\frac{-Ste.t}{3}\right)\right)} \tag{41}$$

A comparison between $u(x,t)$ obtained from MPIM, PSSA, and other iterative methods for $Ste.t$=0.1 and $Ste.t$=1.0 is shown in Figure 5. It is apparent that the results of MPIM are identical to those of PSSA for both values of $Ste.t$, while the results of PIM, VIM, and ADM exhibit varying degrees of deviation from PSSA depending on the magnitude of $Ste.t$. Again, we can see that both boundary conditions are satisfied by MPIM, but the boundary condition at x=0 is not satisfied by ADM, and the boundary condition at x=s is not satisfied by PIM and VIM.

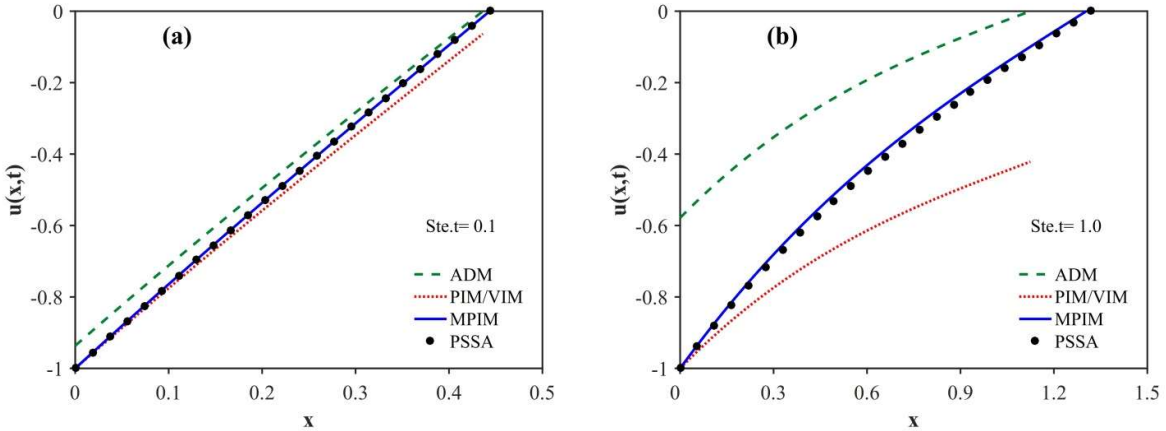

Fig. 5. Results of $u(x,t)$ versus x for the case in which k=1, $f(t)$=-1, α=-Ste and $Ste\rightarrow 0$. (a) $Ste.t$=0.1, (b) $Ste.t$=1.0

In Fig. 6, the moving interface position predicted by MPIM is compared with those obtained by PSSA and other iterative methods. As seen, the results of MPIM show a close match with the results of PSSA, while the results of PIM, VIM, and ADM indicate a growing deviation with increasing the parameter *Ste.t*.

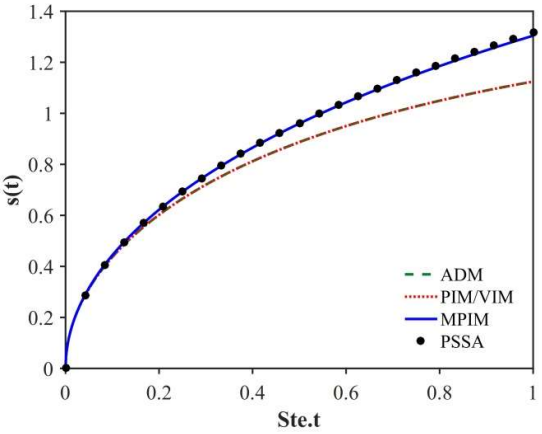

Fig. 6. Results of $s(t)$ versus t for the case in which k=1, $f(t)$=-1, α=-*Ste* and *Ste*→0

3.2. Comparisons with experimental release data

To complete the analysis, the drug release profiles calculated according to the modified Picard iteration method are compared to the experimental data of drug release from halloysite tubules reported in [41]. The halloysite clay, with an average length of 1μm and an inner diameter of 15nm, was loaded with poorly soluble drugs including Dexamethasone, Furosemide, and Nifedipine. The physical properties of these model drugs are presented in Table 2. All release experiments were performed in water at pH 7.4, at room temperature, and under sink conditions.

Table 2. Physical properties of model drugs [42]

Drug	Dexamethasone	Furosemide	Nifedipine
Molecular Weight (g/mol)	392.47	330.74	346.33
Molar Volume (cm^3/mol)	296	206	272
Density (mg/mL)	1300	1600	1350
Solubility in water (mg/mL)	0.10	0.10	0.05
Diffusion coefficient in water* (m^2/s)	4.8×10^{-10}	6.0×10^{-10}	5.1×10^{-10}

* Calculated by Wilke-Chang equation

For this case, the modified Picard iteration method provides the following approximate analytical results for the amount of release:

$$M(t)=\frac{C_s\sqrt{D}}{Ste}\left(\sqrt{\frac{6}{k}}(3+Ste)\tanh^{-1}\left(\sqrt{\frac{k}{6}}s(t)\right)-(2+0.5Ste)s(t)\right) \tag{42}$$

where

$$s(t)=\sqrt{\frac{6}{k}\left(1-exp\left(\frac{-Stekt}{Ste+3}\right)\right)} \tag{43}$$

To obtain the percentage of release, the result of Eq. (42) is divided by M_∞= 0.5mg, which is the amount of drug loaded inside the halloysite tubules. The parameters employed are taken from Table 2, except for D and k, which are found from the model adjustment. Results are illustrated in Fig. 7, and the adjusted parameters are presented in Table 3. For comparison, the results for the cases where $k \rightarrow 0$ are also plotted in Fig. 7 as a dashed line.

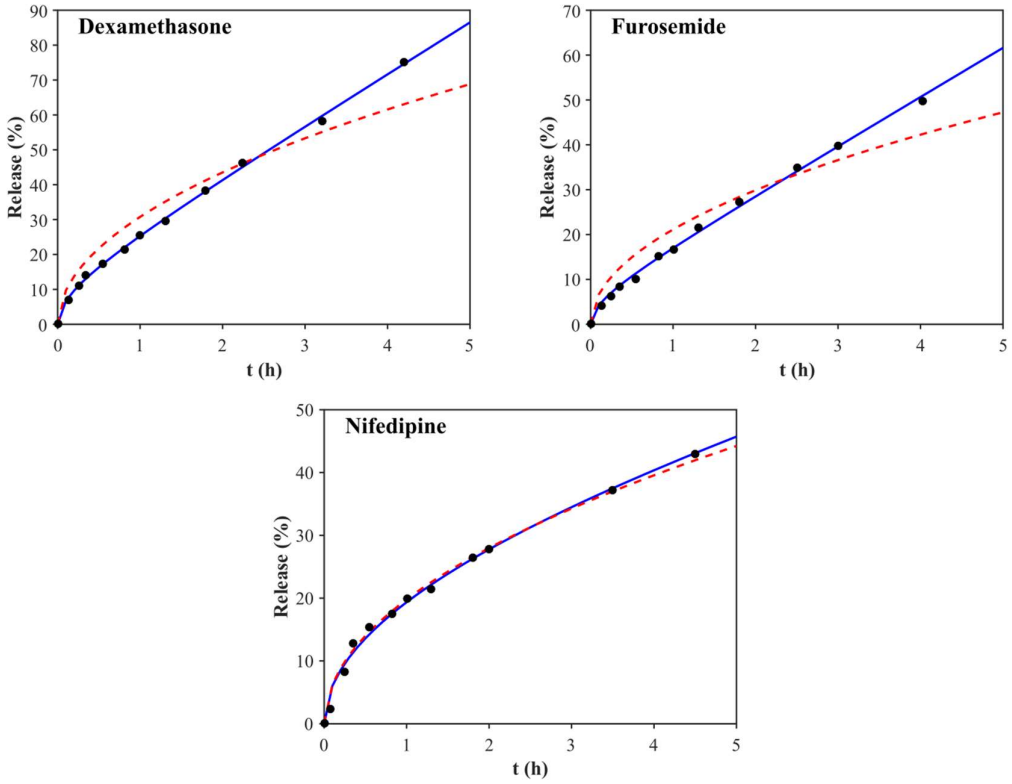

Fig.7. Comparison of release profile calculated according to Eq. (42) (−) and the experimental data reported in [41] (●) for model drug release from halloysite tubules. Dashed line (--) represents results when $k \rightarrow 0$

As seen, Eq. (42) adjusts the experimental drug release very well, but for the case $k \rightarrow 0$, a close match is observed only for Nifedipine. These results indicate that simultaneous dissolution from the moving interface and the perimeter of the pores may be a possible mechanism for the drug release from the halloysite tubules. The small value of k for Nifedipine demonstrates that the dissolution rate from the internal wall of halloysite is low and, therefore, its effect on the release rate is negligible. In contrast, the higher value of k for Dexamethasone and Furosemide shows that the amount of drug dissolved from the internal wall of the halloysite is considerable and causes zero-order release kinetics. The smaller value of k for Nifedipine, compared to its value for Dexamethasone and Furosemide, can be attributed to its lower solubility in water relative to the other two drugs (see Table 2).

Comparing the diffusion coefficients in Table 3 with those in Table 2, it is evident that, despite the differences between the values obtained from curve-fitting and those calculated by the Wilke-Chang equation, all are within the same range of magnitude. The somewhat smaller values of the diffusion coefficients in Table 3, compared to those in Table 2, may be due to the effect of steric hindrance on the diffusion of drug molecules through the liquid-filled pores.

Table 3. The correlation coefficients and fitting parameter of models

Drug	D ($m^2.s^{-1}$)	k (s^{-1})
Dexamethasone	1.9×10^{-10}	2.82
Furosemide	0.9×10^{-10}	4.39
Nifedipine	3.4×10^{-10}	0.42

3.3. Prediction of model

In Fig. 8, Eqs. (42) and (43) are plotted against t for *Ste*=0.1 and 1 and different values of *k*. This figure shows that, at initial times, both the velocity of the moving interface and the release rate depend only on the Stefan number (*Ste*). However, as time progresses, they exhibit a dependency on k. In Fig. 8a, we observe that the velocity of the moving interface is reduced by increasing the value of *k*. This is most evident when the Stefan number is high. When the value of *k* is large, the dissolution rate from the perimeter of pores is high. In this condition, the concentration gradient near the moving boundary is rapidly reduced, causing the velocity of the moving interface to decrease and the moving boundary position to reach a constant value in less time. In Fig. 8b, it is seen that increasing the value of *k* leads to an increase in the release rate. As mentioned before, a high value of *k* means a high dissolution rate from the perimeter of pores. Therefore, the amount of drug entering the pores increases, resulting in a greater release rate. At long times, the dissolution from the perimeter of pores prevails over the dissolution from the moving interface. Hence, as seen in Fig. 8b, the release rate becomes constant (zero order).

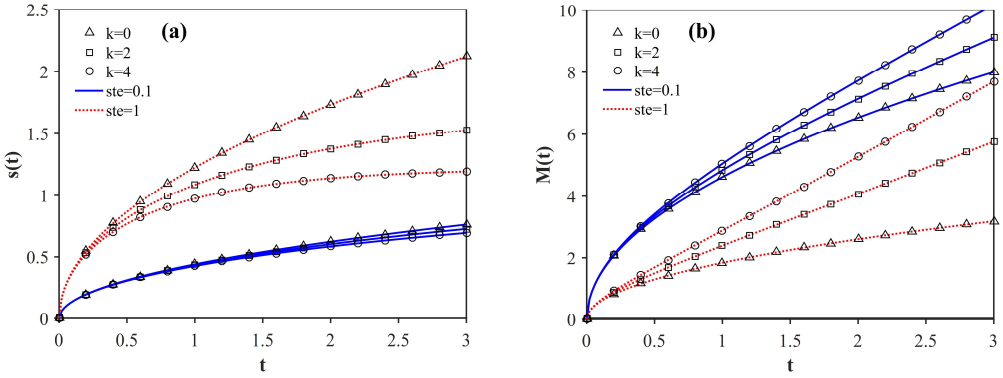

Fig. 8. Results of (a) position of moving interface $s(t)$, (b) amount of release $M(t)$ versus t for *Ste* and *k*

4. Conclusion

In this paper, the modified Picard iteration method (MPIM) was proposed for solving one-dimensional moving boundary problems with Dirichlet boundary conditions. For the cases evaluated in this study, MPIM provides more accurate results than PIM, VIM, and ADM. It remains to be examined whether MPIM is superior to other iterative methods for problems with non-Dirichlet boundary conditions. As observed, one iteration of MPIM yields results close to the exact solutions. However, if more precise results are required, additional iterations should be performed. Sometimes, it is possible to obtain the complete series of the solution via mathematical induction, which may converge to the exact solution if it exists. The present method may also be of interest for solving two- and three-dimensional moving boundary problems.

References

[1] Garshasbi, M., Dastour, H., 2016. A mollified marching solution of an inverse ablation-type moving boundary problem. Computational and Applied Mathematics, 35(1), 61-73. https://doi.org/10.1007/s40314-014-0180-5
[2] Singh, A.K., Kumar, A., Rajeev. 2019. A Stefan problem with variable thermal coefficients and moving phase change material. Journal of King Saud University - Science, 31(4), 1064-1069. https://doi.org/10.1016/j.jksus.2018.09.009
[3] Beiranvand, A., Ivaz, K., 2014. Solving the Stefan Problem with Kinetics. Computational Methods for Differential Equations, 2(1), 37-49.
[4] Crank, J., 1987. Free and Moving Boundary Problems, Clarendon Press, Oxford shire: New York, p. 424.
[5] Kim, S.H., 2014. Two Simple Numerical Methods for the Free Boundary in One-Phase Stefan Problem. Journal of Applied Mathematics, 2014, 1-10. https://doi.org/10.1155/2014/764532
[6] Sadoun, N., Si-Ahmed, E.-K., Colinet, P., Legrand, J., 2012. On the boundary immobilization and variable space grid methods for tra nsient heat conduction problems with phase change: Discussion and refinement. Comptes Rendus Mécanique, 340(7), 501-511. https://doi.org/10.1016/j.crme.2012.03.003
[7] Karabenli, H., Uçar, Y., Aksan, N., 2016. A collocation finite element solution for Stefan problems with periodic boundary conditions. Filomat, 30(3), 699-709. https://doi.org/10.2298/FIL1603699K
[8] Ivanovic, M., Svicevic, M., Savovic, S., 2017. Numerical solution of Stefan problem with variable space grid method based on mixed finite element/finite difference approach. International Journal of Numerical Methods for Heat & Fluid Flow, 27(12), 2682-2695. https://doi.org/10.1108/HFF-11-2016-0443
[9] Singh, J., Jitendra, Rai, K.N., 2020. Legendre wavelet based numerical solution of variable latent heat moving boundary problem. Mathematics and Computers in Simulation, 178, 485-500. https://doi.org/10.1016/j.matcom.2020.06.020
[10] Chaurasiya, V., Chaudhary, R.K., Awad, M.M., Singh, J., 2022. A numerical study of a moving boundary problem with variable thermal c onductivity and temperature-dependent moving PCM under periodic boundary condition. The European Physical Journal Plus, 137(6), 714. https://doi.org/10.1140/epjp/s13360-022-02927-w
[11] Lee, P.I., 2011. Modeling of drug release from matrix systems involving moving boundaries: Approximate analytical solutions. International Journal of Pharmaceutics, 418(1), 18-27. https://doi.org/10.1016/j.ijpharm.2011.01.019
[12] Fazli-Abukheyli, R., Rahimi, M.R., Ghaedi, M., 2020. Experimental study and modeling of in vitro agrochemicals release from nanoporous anodic alumina. Chemical Papers. https://doi.org/10.1007/s11696-019-01045-9
[13] Yu, Z.-T., Fan, L.-W., Hu, Y.-C., Cen, K.-F., 2010. Perturbation solution to heat conduction in melting or solidification with heat generation. Heat and Mass Transfer, 46(4), 479-483. https://doi.org/10.1007/s00231-010-0596-4
[14] Parhizi, M., Jain, A., 2019. Solution of the Phase Change Stefan Problem with Time-Dependent Heat F lux Using Perturbation Method. Journal of Heat Transfer, 141(2), 024503. https://doi.org/10.1115/1.4041956
[15] Bollati, J., Natale, M.F., Semitiel, J.A., Tarzia, D.A., 2018. Integral balance methods applied to a non-classical Stefan problem. https://doi.org/10.2298/TSCI180901310B
[16] Ribera, H., Myers, T.G., MacDevette, M.M., 2019. Optimising the heat balance integral method in spherical and cylindric al Stefan problems. Applied Mathematics and Computation, 354, 216-231. https://doi.org/10.1016/j.amc.2019.02.039
[17] Wood, A.S., 2001. A new look at the heat balance integral method. Applied Mathematical Modelling, 25(10), 815-824. https://doi.org/10.1016/S0307-904X(01)00016-6
[18] Sadoun, N., Si-Ahmed, E.-K., Colinet, P., 2006. On the refined integral method for the one-phase Stefan problem with t ime-dependent boundary conditions. Applied Mathematical Modelling, 30(6), 531-544. https://doi.org/10.1016/j.apm.2005.06.003
[19] Myers, T.G., 2010. Optimal exponent heat balance and refined integral methods applied to Stefan problems. International Journal of Heat and Mass Transfer, 53(5), 1119-1127. https://doi.org/10.1016/j.ijheatmasstransfer.2009.10.045
[20] Mennig, J., Özişik, M.N., 1985. Coupled integral equation approach for solving melting or solidification. International Journal of Heat and Mass Transfer, 28(8), 1481-1485. https://doi.org/10.1016/0017-9310(85)90250-9
[21] Sudhakar, B., 1992. On integral iterative formulations in classical Stefan problems. Chemical Engineering Science, 47(12), 3158-3162. https://doi.org/10.1016/0009-2509(92)87020-Q
[22] Sudhakar, B., 1992. An integral method for non-linear moving boundary problems. Chemical Engineering Science, 47(2), 475-479. https://doi.org/10.1016/0009-2509(92)80035-B
[23] Rajeev, Kushwaha, M.S., 2013. Homotopy perturbation method for a limit case Stefan problem governed by fractional diffusion equation. Applied Mathematical Modelling, 37(5), 3589-3599. https://doi.org/10.1016/j.apm.2012.07.047
[24] Slota, D., 2010. The application of the homotopy perturbation method to one-phase inverse Stefan problem. International Communications in Heat and Mass Transfer, 37(6), 587-592. https://doi.org/10.1016/j.icheatmasstransfer.2010.03.009
[25] Słota, D., Chmielowska, A., Brociek, R., Szczygieł, M., 2020. Application of the Homotopy Method for Fractional Inverse Stefan Probl em. Energies, 13(20), 5474. https://doi.org/10.3390/en13205474
[26] Hetmaniok, E., Słota, D., Wituła, R., Zielonka, A., 2011. Comparison of the Adomian decomposition method and the variational ite ration method in solving the moving boundary problem. Computers & Mathematics with Applications, 61(8), 1931-1934. https://doi.org/10.1016/j.camwa.2010.07.050
[27] Qin, X.-Y., Duan, Y.-X., Yin, M.-R., 2014. Approximate Analytic Solutions for the Two-Phase Stefan Problem Using the Adomian Decomposition Method. Journal of Applied Mathematics, 2014, 1-6. https://doi.org/10.1155/2014/391606

[28] Słota, D., 2007. Direct and inverse one-phase Stefan problem solved by the variational iteration method. Computers & Mathematics with Applications, 54(7-8), 1139-1146. https://doi.org/10.1016/j.camwa.2006.12.061
[29] Witula, R., Hetmaniok, E., Slota, D., Zielonka, A., 2010. Application of the Picard's Iterative Method for the Solution of One-P hase Stefan Problem. Archives of Foundry Engineering, 10 (sp. is. ~4), 83-88.
[30] Witula, R., Hetmaniok, E., Slota, D., Zielonka, A., 2011. Solution of the two-phase Stefan problem by using the Picard's iterati ve method. Thermal Science, 15(suppl. 1), 21-26. https://doi.org/10.2298/TSCI11S1021W
[31] Higuchi, T., 1961. Rate of release of medicaments from ointment bases containing drugs in suspension. Journal of Pharmaceutical Sciences, 50(10), 874-875. https://doi.org/10.1002/jps.2600501018
[32] Paul, D.R., McSpadden, S.K., 1976. Diffusional release of a solute from a polymer matrix. Journal of Membrane Science, 1, 33-48. https://doi.org/10.1016/s0376-7388(00)82256-5
[33] Lee, P.I., 1980. Diffusional release of a solute from a polymeric matrix — approximate analytical solutions. Journal of Membrane Science, 7(3), 255-275. https://doi.org/10.1016/s0376-7388(00)80472-x
[34] Abdekhodaie, M.J., Cheng, Y.L., 1997. Diffusional release of a dispersed solute from planar and spherical matrices into finite external volume. Journal of Controlled Release, 43(2), 175-182. https://doi.org/10.1016/s0168-3659(96)01482-4
[35] Cohen, D.S., Erneux, T., 1998. Controlled Drug Release Asymptotics. SIAM Journal on Applied Mathematics, 58(4), 1193-1204. https://doi.org/10.1137/S0036139995293269
[36] Jain, A., McGinty, S., Pontrelli, G., 2022. Drug diffusion and release from a bioerodible spherical capsule. International Journal of Pharmaceutics, 616, 121442. https://doi.org/10.1016/j.ijpharm.2021.121442
[37] Garshasbi, M., Malek Bagomghaleh, S., 2022. On a moving boundary problem associated with the swelling drug release platforms. International Journal of Computer Mathematics, 99(12), 2499-2523. https://doi.org/10.1080/00207160.2022.2069466
[38] Robin, W.A., 2010. Solving differential equations using modified Picard iteration. International Journal of Mathematical Education in Science and Technol ogy, 41(5), 649-665. https://doi.org/10.1080/00207391003675182
[39] Mani, G., Macias, C.E., Feldman, M.D., Marton, D., Oh, S., Mauli Agrawal, C., 2010. Delivery of paclitaxel from cobalt–chromium alloy surfaces without polymeric carriers. Biomaterials, 31(20), 5372-5384. https://doi.org/10.1016/j.biomaterials.2010.03.043
[40] Zhang, Y., He, F., Sun, Z., Li, L., Huang, Y., 2014. Controlled delivery of dexamethasone from TiO_2 film with nanoporous structure on Ti–25Nb–3Mo–2Sn–3Zr biomedical alloy without polymeric carrier. Materials Letters, 128, 384-387. https://doi.org/10.1016/j.matlet.2014.04.149
[41] Veerabadran, N.G., Price, R.R., Lvov, Y.M., 2007. Clay nanotubes for encapsulation and sustained release of drugs. Nano, 02(02), 115-120. https://doi.org/10.1142/s1793292007000441
[42] Elumalai, D.N., Lvov, Y., Derosa, P., 2015. Implementation of a Simulation Model of the Controlled Release of Molecular Species from Halloysite Nanotubes. Journal of Encapsulation and Adsorption Sciences, 05(01), 74-92. https://doi.org/10.4236/jeas.2015.51006

Appendix

Variation iteration method:

$$u_0(x,t) = f(t)\left(1-\frac{x}{s(t)}\right)$$

$$u_{m+1}(x,t) = u_m(x,t) + \int_0^x (x-z)\left(\frac{\partial u_m(z,t)}{\partial t} + k u_m(z,t) - \frac{\partial^2 u_m(z,t)}{\partial z^2}\right) dz, m = 0,1,2,3,\ldots$$

$$u_1(x,t) = f(t) - \left(\frac{f(t)}{s(t)}\right)x + \left(\frac{kf(t) + \frac{df(t)}{dt}}{2}\right)x^2 + \left(\frac{f(t)\frac{ds(t)}{dt} - s(t)\frac{df(t)}{dt} - kf(t)s(t)}{6s(t)^2}\right)x^3$$

$$s_1(t) = \sqrt{\frac{4\alpha\int_0^t \frac{f(\tau)g(\tau)}{\alpha f(\tau)+2}d\tau}{g(t)}} \quad \text{where} \quad g(t) = exp\left(2\alpha\int_0^t \frac{\left(kf(\tau) + \frac{df(\tau)}{d\tau}\right)}{\alpha f(\tau)+2} d\tau\right)$$

Picard iteration method:

$$u_0(x,t)=f(t)\left(1-\frac{x}{s(t)}\right)$$

$$u_{m+1}(x,t)=\left(\frac{\partial u_m(0,t)}{\partial x}\right)x+u(0,t)+\int_0^x(x-z)\left(\frac{\partial u_m(z,t)}{\partial t}+ku_m(z,t)\right)dz, m=0,1,2,3,...$$

$$u_1(x,t)=f(t)-\left(\frac{f(t)}{s(t)}\right)x+\left(\frac{kf(t)+\frac{df(t)}{dt}}{2}\right)x^2+\left(\frac{f(t)\frac{ds(t)}{dt}-s(t)\frac{df(t)}{dt}-kf(t)s(t)}{6s(t)^2}\right)x^3$$

$$s_1(t)=\sqrt{\frac{4\alpha\int_0^t\frac{f(\tau)g(\tau)}{\alpha f(\tau)+2}d\tau}{g(t)}} \text{ where } g(t)=exp\left(2\alpha\int_0^t\frac{\left(kf(\tau)+\frac{df(\tau)}{d\tau}\right)}{\alpha f(\tau)+2}d\tau\right)$$

Adomian decomposition method:

$$u_m(x,t)=\sum_{i=0}^m h_i(x,t), m=0,1,2,3,...$$

$$h_0(x,t)=f(t)\left(1-\frac{x}{s(t)}\right)$$

$$h_{m+1}(x,t)=\int_x^{s(t)}\int_x^0\left(\frac{\partial h_m(z,t)}{\partial t}+kh_m(z,t)\right)dzdz$$

$$u_1(x,t)=\frac{-f(t)}{s(t)}\left(x-s(t)\right)+\left(\frac{kf(t)+\frac{df(t)}{dt}}{2}\right)\left(x^2-s(t)^2\right)+\left(\frac{f(t)\frac{ds(t)}{dt}-s(t)\frac{df(t)}{dt}-kf(t)s(t)}{6s(t)^2}\right)\left(x^3-s(t)^3\right)$$

$$s_1(t)=\sqrt{\frac{4\alpha\int_0^t\frac{f(\tau)g(\tau)}{\alpha f(\tau)+2}d\tau}{g(t)}} \text{ where } g(t)=exp\left(2\alpha\int_0^t\frac{\left(kf(\tau)+\frac{df(\tau)}{d\tau}\right)}{\alpha f(\tau)+2}d\tau\right)$$